VII. MICROWAVE TUBE RESEARCH

L. D. Smullin
Prof. L. J. Chu
Dr. H. A. Haus
A. Bers
D. L. Bobroff
C. Fried
A. J. Lichtenberg
H. Shelton

A. NOISE REDUCTION BY MEANS OF A LOSSY BEAM TRANSFORMER

The minimum noise figure of a traveling-wave tube obtainable by means of lossless beam transformers has been found (1) to be

$$F_{min} = 1 + \frac{4\pi}{kT} (4QCf_{max} f_{min})^{1/2} (S_o - \Pi_o) \qquad (1)$$

where

$$S_o = \left(\Phi_o \Psi_o - \Lambda_o^2\right)^{1/2}$$

in which Φ_o is the self power spectrum of the noise voltage, Ψ_o is the self power spectrum of the noise current, Λ_o is the imaginary part of the cross power spectrum of the noise voltage and current, and Π_o is the real part of the cross power spectrum; the subscript o indicates that all noise power spectra are taken at a reference plane beyond the potential minimum in the electron gun. The reference plane is chosen sufficiently far from the potential minimum that an approximate single velocity treatment of the electron flow is justified at and beyond the reference plane. In other words, the average velocity of the electrons at the reference plane must be large compared to their velocity spread.

If the corresponding power spectra at an arbitrary cross-sectional plane of the electron beam are indicated by Φ, Ψ, Λ, and Π, and if we set $S = (\Phi\Psi - \Lambda^2)^{1/2}$, then $S = S_o$ and $\Pi = \Pi_o$, as proved before (1), provided only lossless beam transformers act upon the beam. Velocity jumps, beam expansions and contractions, and the like, if analyzed under the assumption of a one-dimensional geometry, are examples of lossless beam transformers.

It is of interest to know whether or not an extraction of noise power from the electron beam would lead to a lower ultimate noise figure than that given in Eq. 1.

A wide class of microwave structures that extract rf power from an electron beam can be represented as lossy nonreciprocal four-terminal networks so far as their

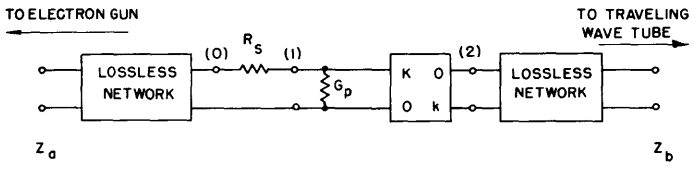

Fig. VII-1
Equivalent circuit of a lossy nonreciprocal four-terminal network.

action upon the rf beam voltage and current is concerned. A helix terminated in passive loads at both ends is an example of such a structure (2). It has been proved that the action of a lossy beam transformer upon a beam before it enters the amplifier structure cannot improve the noise figure of a traveling-wave tube below the limit given in Eq. 1. The proof is summarized below.

The most general nonreciprocal lossy four-terminal network can be represented by an equivalent circuit (3) as shown in Fig. VII-1. The amplifier (or attenuator) characterized by the matrix of the generalized circuit parameters (4)

$$\begin{bmatrix} k & o \\ o & k \end{bmatrix}$$

has an amplification (or attenuation) k which is limited by the inequality

$$\frac{1}{2}\left(k + \frac{1}{k}\right) \leq (R_s G_p + 1)^{1/2}$$

The noise parameters S_o and Π_o which are fed into the network at the point z_a appear at the output terminals at z_b as S_2 and Π_2. The difference $S_2 - \Pi_2$ enters into the expression for the minimum obtainable noise figure of a traveling-wave tube whose rf structure follows the beam transformer at $z > z_b$. It is proved that the extraction of rf power from the beam does not improve the noise figure of a traveling-wave tube below the limit given in Eq. 1 if it is shown that $\left[(S_2 - \Pi_2)/(S_o - \Pi_o)\right] \geq 1$ for any choice of the network and for any noise characteristics. If one expresses the parameters S_o and Π_o, S_2 and Π_2, in terms of the power spectra Φ_1, Ψ_1, Λ_1, and Π_1 at the point 1 in the equivalent circuit of Fig. VII-1, one finds

$$\frac{S_2 - \Pi_2}{S_o - \Pi_o} = k^2 \frac{\left(1 + \frac{G_p^2 \Phi_1^2}{S_1^2} - 2\frac{G_p \Phi_1}{S_1}\frac{\Pi_1}{S_1}\right)^{1/2} - \frac{\Pi_1}{S_1}\frac{G_p \Phi_1}{S_1}}{\left(1 + \frac{R_s^2 \Psi_1^2}{S_1^2} + 2\frac{R_s \Psi_1}{S_1}\frac{\Pi_1}{S_1}\right)^{1/2} - \frac{\Pi_1}{S_1} - \frac{R_s \Psi_1}{S_1}}$$

This expression can be minimized with respect to $(R_s \Psi_1)/S_1$, $(G_p \Phi_1)/S_1$, and $R_s G_p$, keeping in mind that $\Psi_1 = \left(S_1^2 + \Lambda_1^2\right)/\Phi_1 \geq S_1^2/\Phi_1$, according to the definition of the noise parameter S. The minimization corresponds to a proper choice of the transformer network. We find that the minimum of the right-hand side of Eq. 3 is equal to unity, independent of the parameter Π_1/S_1, that is, independent of the character of the noise in the beam.

In conclusion, the following statement can be made: Under the assumption that a one-dimensional analysis of the electron beam is justified, a lossy "four-terminal" beam transformer preceding the amplifier structure of a traveling-wave tube cannot

lower the noise figure of the traveling-wave tube below the value given in Eq. 1. This value is fixed entirely by the noise process between the cathode and a reference plane beyond the potential minimum in the electron gun.

H. A. Haus

References

1. Quarterly Progress Report, Research Laboratory of Electronics, M.I.T., April 15, 1954.

2. H. Schnittger, D. Weber, Fernmelde Technische Zeitschrift, 7, 302 (1953).

3. H. A. Haus, Paper to be published in the Journal of Applied Physics.

4. E. A. Guillemin, Communication Networks (John Wiley and Sons, New York, 1931).

B. NOISE-REDUCTION SYSTEMS

1. Optimum Space-Charge Regions

The noise-reduction factor of a general accelerating region, operating on a noise space-charge wave of infinite standing-wave ratio (see the Quarterly Progress Report, April 15, 1954), has been optimized with respect to the parameter y_1^*. Physically this corresponds to adjusting the "input ratio" $y_1 = |J_1/V_1|$ of the region to obtain a maximum noise reduction.

Figures VII-2 and VII-3 show the results graphically. For a chosen set of $\delta = u_2/u_1$ and ζ the physical structure of the region is fixed. To such a point in Fig. VII-2 there correspond optimum rf input conditions to the region which are specified by $y^*_{1\,opt}$. (Figure VII-3 is an example of the variation of $y^*_{1\,opt}$ for the case of a space-charge-limited region.)

Hence, the dc parameters δ and ζ of an accelerating region, together with the corresponding optimum rf input conditions, determine the optimum noise reduction factor $r_{1\,min}$ of such a region.

The actual input conditions are obtained from the input ratio

$$y_{1\,opt} = \left|\frac{J_1}{v_1}\right|_{opt} = \omega\left(\frac{2\epsilon}{\eta}\right)^{1/2}\left(\zeta\,\frac{\delta+1}{\delta}\right)^{1/2}\left(\frac{J_o}{u_2}\right)^{1/2} y^*_{1\,opt}$$

This optimum "input ratio" is then realizable by a proper drift region preceding the chosen accelerating region.

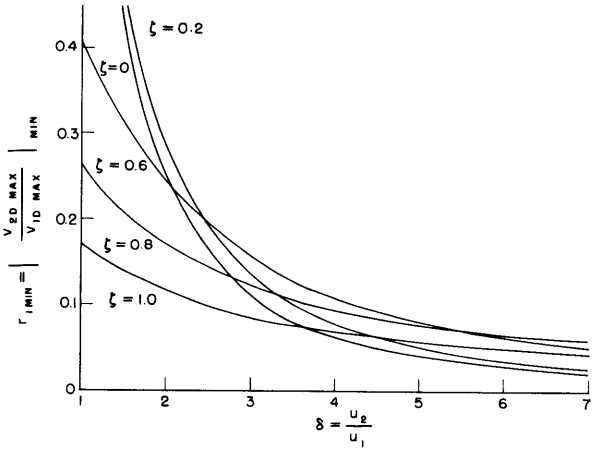

Fig. VII-2
Minimum noise reduction factor vs velocity ratio (y_1^* optimized).

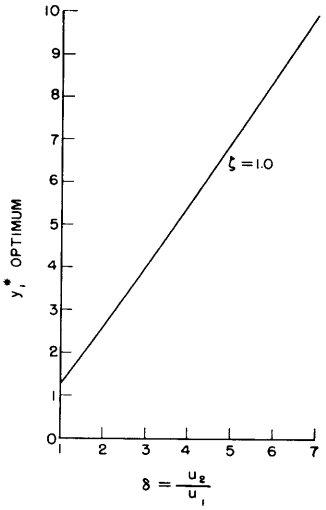

Fig. VII-3
Optimum input conditions for a space-charge-limited region.

The important new result is that a space-charge-limited accelerating region, $\zeta = 1$, has the lowest noise reduction factor for δ's up to 3.6 (a voltage increase of 13 times). Only for velocity ratios greater than 3.6 will the velocity jump, $\zeta = 0$, give better noise reduction.

2. Regions of Constant Acceleration

These regions are characterized by the fact that there is no space charge, $\zeta = 0$, and hence the electron velocity increases linearly. Although this may be considered as a special case of the general region investigated above, due attention must be given to the electronic equations used. Since the Llewellyn-Peterson equations are space-charge equations, for the case of no space charge they will apply only if the length of the region is short as compared with the space-charge wavelength.

Under such conditions, the constant accelerating region of finite transit time was analyzed for its noise-reduction properties. The noise-reduction factor (see the Quarterly Progress Report, April 15, 1954) was found to be

$$r_1 = \frac{1}{\delta^2} \frac{(1 - cz_1y_1)^2 + \delta^3 z_1^2 y_1^2}{z_1^2 y_1^2 + 1}$$

where $y_1 = |J_1/v_1|$; $\delta = u_2/u_1$; $z_1 = (u_1/J_o)(\omega_{q1}/\omega)$; and $c = x/\lambda_{q1}$ must be a constant, small compared to 1/4 (x is the distance between electrodes; λ_{q1} is the space-charge wavelength at the first electrode).

Minimization of r_1 with respect to y_1 yielded

$$r_{1\,\min} \approx \frac{1}{\delta^2}\left(1 - \frac{c^2}{\delta^3}\right); \quad \delta^3 >> 1; \quad c < \frac{1}{4}$$

with the corresponding optimum "input ratio"

$$y_{1\,\mathrm{opt}} \approx \frac{c}{z_1(\delta^3 + c^2 - 1)}$$

These equations show that a finite length (but short compared to $\lambda_{q1}/4$) $\zeta = 0$ region can be made to give noise reductions at least as good as a velocity jump ($c = 0$), by properly adjusting the input conditions.

A. Bers

C. EXAMINATION OF ASSUMPTIONS IMPLIED IN PREDICTED MINIMUM NOISE FIGURE FOR TRAVELING-WAVE TUBES

Watkins (1) and later Pierce (2) predicted a minimum noise figure for traveling-wave tubes of 6 db. Implied in these predictions are the following assumptions: (a) excitation of only the fundamental beam mode of propagation; (b) no coupling of beam modes in the electron gun; (c) no space-charge smoothing or related phenomena at microwave frequencies.

The first assumption is known to be in error. In previous work, Rowe (3) showed that the higher modes of propagation will be excited to an appreciable extent. According to Rowe's theory only about two-thirds of the noise power at the cathode goes into the first mode, the remainder into the higher modes. This fact should result in a noise figure lower than that predicted, since the higher modes couple less strongly to the helix than the fundamental. To obtain the theoretical minimum noise figure, however, the beam must be acted upon by velocity jumps and accelerating regions that reduce the effect of the fundamental mode but are apt to act adversely on the higher modes and enhance their otherwise negligible contribution to the noise figure. In the light of these considerations, the inclusion of the effect of the noise in at least the second mode seems warranted in traveling wave tube noise calculations.

While the beam modes (4) in an unaccelerated ion-neutralized electron beam are essentially orthogonal, this is not the case in regions where dc acceleration occurs; the beam modes will be coupled to a certain extent. An estimate of the amount of mode coupling to be expected can be obtained by computing the coupling that takes place in velocity jumps. For a parallel beam in an infinite magnetic field, a good approximation to the amount of coupling that takes place in a velocity jump can easily be determined by expanding the ac velocity (or current) distribution of the modes before the jump in terms

Table I

Beam Mode Coupling in Velocity Jump 40 Volts to 640 Volts. Beam Diameter, 1 mm. Infinite Magnetic Field.

Modes After Jump	Modes Before Jump Normalized to 1			
	1st	2nd	3rd	4th
1st	0.812	-0.068	0.019	0.008
2nd	0.249	0.968	-0.070	0.024
3rd	-0.095	0.138	0.991	0.054
4th	0.054	-0.061	0.087	0.992

Table II

Beam Mode Coupling in Velocity Jump 640 Volts to 40 Volts. Beam Diameter, 1 mm. Infinite Magnetic Field.

Modes After Jump	Modes Before Jump Normalized to 1			
	1st	2nd	3rd	4th
1st	1.198	0.088	-0.019	0.007
2nd	-0.294	0.998	0.080	-0.024
3rd	0.149	-0.128	0.995	0.061
4th	-0.092	0.064	-0.078	0.993

of the velocity (or current) distributions of the modes after the jump. The results of such computations for two specific cases are summarized in Tables I and II. The coupling of each of the first four modes before the jump to the first four modes after the jump is given. The two velocity jumps are perhaps extreme cases and give estimates of the upper limits to the amount of coupling that will occur between modes in the pre-helix region of traveling-wave tubes. Tables I and II indicate that the coupling of the first mode before the velocity jump with the second mode after the jump may be as high as 25 percent.

In performing these computations an infinite magnetic field was assumed to prevent lateral motion of the electrons. A more refined computation is planned which will include the electrostatic lens action of the accelerating region in finite magnetic fields.

The correctness of the assumption of no space-charge smoothing at microwave frequencies cannot be determined until a knowledge of the mechanism of space-charge smoothing is attained. The existence of space-charge smoothing at low frequencies has been established both experimentally and theoretically. While the theory does not lead immediately to a clear understanding of the mechanism of space-charge smoothing, it does seem to indicate that an excess of electrons in one velocity group temporarily lowers the potential minimum and thereby reduces the number of electrons in all velocity groups so that, on the average, the original excess charge is almost cancelled. Most of the remanent noise seems to be caused by the velocity modulation introduced by the difference in the velocity of the original excess charge and the mean velocity of the compensating charge. If we assume that the mechanism of space-charge smoothing is as outlined above, a relaxation time for the space charge smoothing process can be obtained on the basis of an admittably questionable assumption. Our purpose is to get a dimensionally correct expression that is closely related to the assumed process of space-charge smoothing.

We adopt a one-dimensional picture of the region between the cathode and anode. The dc current is assumed to be space-charge-limited so that a virtual cathode exists a very short distance in front of the actual cathode. The dc current density is then

$$I_o = I_c \exp(-e V_{mo}/kT_c)$$

where I_c is the average current density emitted from the cathode, V_{mo} is the potential of the virtual cathode relative to the real cathode, and T_c is the cathode temperature. A short pulse of "sheet" electrons with a velocity sufficient to get past the space-charge minimum and total surface charge density $-q_1$ is emitted from the cathode into the otherwise steady-state space-charge-limited current. A positive surface charge density q_1, the image of $-q_1$, is left behind on the cathode. An electric field approximately equal to q_1/ϵ_o then extends between q_1 and $-q_1$. This field will undoubtedly be modified by the steady-state space charge but in order to obtain a result without solving the space-charge problem we assume that such is not the case. The lowering of the potential minimum immediately after the passage of $-q_1$ through it will be given by $V_{m1} \approx q_1/\epsilon_o X_m$ where X_m is the distance of the virtual cathode from the real cathode. We now assume that this results in a modified current density

$$I_o + I_1 = I_c \exp\left[-e(V_{om} + V_{1m})/kT_c\right]$$

which gives

$$I_1 \approx -I_o \frac{e V_{1m}}{kT_c}$$

The value of V_{lm} will, of course, decrease towards zero as the field of the charge carried across by I_l cancels the field of the original excess charge. Nevertheless, in the spirit of the present approximate analysis, we assume V_{lm}, and hence I_l, to be constant until sufficient charge crosses the minimum to neutralize $-q_l$ and then drops immediately to zero. The time required for this to take place should yield a rough estimate of the relaxation time for the space charge smoothing process provided, of course, that the assumed mechanism of space-charge smoothing is the correct one. This time is

$$\tau = \frac{q_l}{I_l} = \frac{kT_c}{I_o}\left(\frac{\epsilon_o}{e\,X_m}\right)$$

with $X_m = 0.002$ cm, $T_c = 1000°K$, $I_o = 1$ ma/mm^2, $\tau \approx 10^{-10}$ sec. This result indicates that space-charge smoothing for frequencies up to approximately 3×10^9 cps cannot be ruled out entirely and that a more accurate analysis is required. Of importance, too, is the fact that the transit time of electrons from the cathode to the virtual cathode is also of the order of 10^{-10} sec so that an excessive delay in the onset on the supposed space charge mechanism will not be caused by this factor.

D. L. Bobroff

References

1. D. A. Watkins, Technical Report No. 31, Electronics Research Laboratory, Stanford University, California, March 15, 1951.

2. J. R. Pierce, Paper to be published in the Journal of Applied Physics.

3. H. E. Rowe, Sc. D. Thesis, M.I.T. (1952).

4. S. Ramo, Proc. I.R.E. 27, 757 (1939).

D. NOISE IN ELECTRON BEAMS

1. Low-Noise Gun Design

Noise measurements have been performed on a low-noise three-region gun developed by R. W. Peter (1). The specifications supplied with the gun indicated the following operating conditions: cathode temperature, 1050-1100°C; cathode current, 300 μa; beam-forming electrode voltage, 0 volts; first anode voltage, 37 volts; second anode voltage, 110 volts; third anode voltage, 530 volts; magnetic field, 455 gauss. It was found, however, that with the voltages given above the beam current was approximately 25 percent more. No current was intercepted by any of the electrodes.

Figure VII-4 shows a number of noise-current curves as functions of distance along the drift tube.

In all of these curves the cathode temperature, the beam-forming electrode voltage, and the first anode voltage were adjusted to the prescribed values. For one of the curves, the other parameters correspond to the specifications supplied. For the other curves, however, either the second or the third anode voltage differed from the recommended data. The essential characteristics of the noise-current curves may be summarized as follows. The noise-current maxima were at least 19 db below the pure shot noise level, provided the second anode voltage was not grossly misadjusted. Under the same conditions, the standing-wave ratio did not exceed 7 db. By suitably adjusting the second anode voltage, the standing-wave ratio could be reduced to approximately 1.5 db. The indications were that with a few more trials even further reductions could have been obtained. Under most conditions, the product $I_{max}I_{min}$ remained remarkably constant at 22 $\pm$ 1 db. Exceptions occurred when the second and third anodes, or the second anode and cathode were tied together; the resulting product of $I_{max}I_{min}$ then became 19 $\pm$ 0.5 db and 17 $\pm$ 0.5 db, respectively. In both cases, however, the collector current changed by approximately 15 percent. According to a recent, somewhat restricted, theory of Pierce (2) and a more general one of Haus (3), the product $K_d I_{max} I_{min}$ must be conserved as long as no rf power is added to or subtracted from the beam. Here, K_d is the impedance of the beam; I_{max} and I_{min} denote the noise-current maximum and minimum, respectively. Further experiments will be made to test this theory.

2. Interception Current

A number of measurements have been performed in an effort to determine the effect of interception current upon the noise in electron beams. The prevailing explanation and treatment of partition noise is due to North (4). For complete space charge smoothing Γ^2 is very small, and the partition noise can be described according to North's formula as follows:

$$\overline{i_n^2} \approx \frac{I_c - I_n}{I_c} \times 2eI_n\Delta f \qquad (1)$$

The factor $(I_c - I_n)/I_c$ represents the fraction of the cathode current that does not reach the n^{th} collector. In a traveling-wave tube, I_n would represent the collector current; $(I_c - I_n)/I_c$, the interception current. If, in a traveling-wave tube, the interception occurs before the beam enters the circuit, the beam current passing through the circuit contains an additional noise current. This noise current is uncorrelated with the noise currents and velocities otherwise contained by the beam.

The effect of interception current was determined experimentally, first, with the parallel gun described in the Quarterly Progress Report of October 15, 1953.

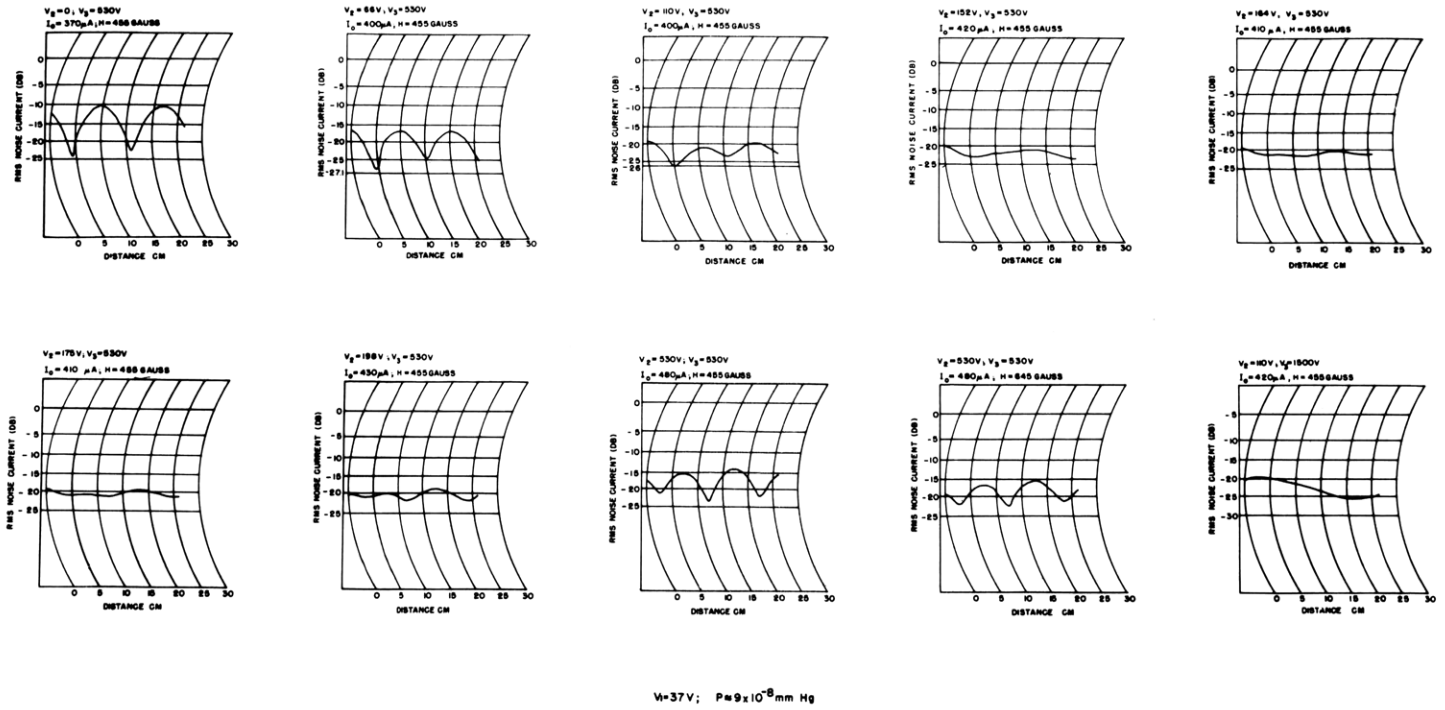

Fig. VII-4

Noise current vs cavity position for the low-noise three-region gun.

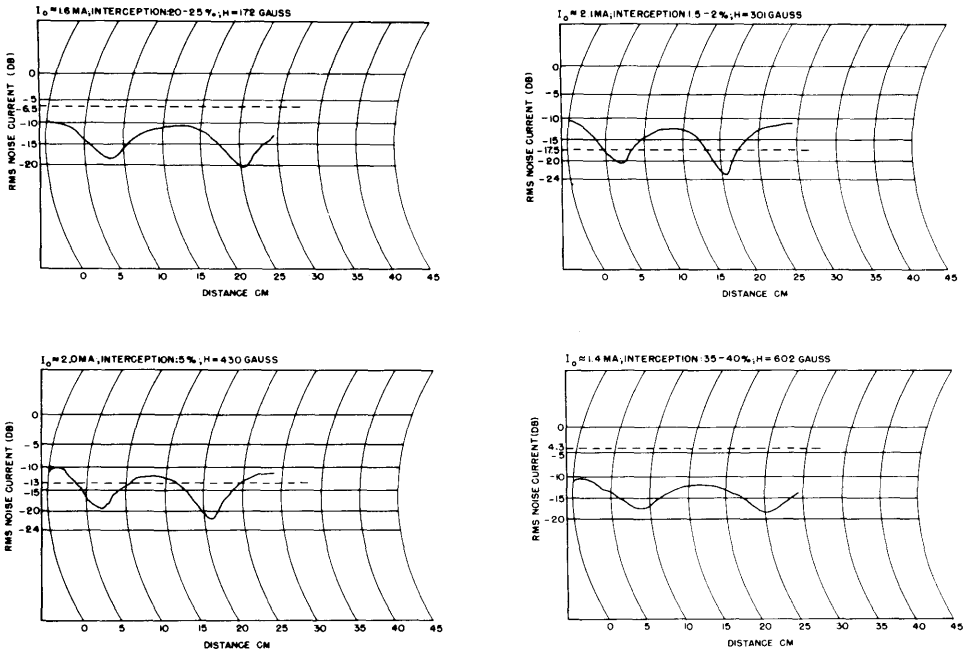

V_o = 1500 V; P ~ 2×10^{-7} mm Hg

Fig. VII-5

Noise current vs cavity position of a confined-flow beam with large interception current.

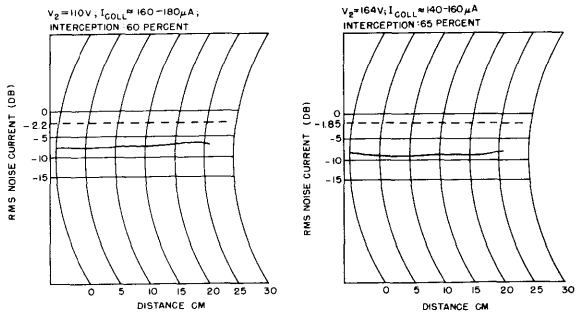

Fig. VII-6

Noise current vs cavity position, using the three-region gun with large interception current. V_1 = 37 volts; V_3 = 530 volts; H = 455 gauss; p ≈ 8.5×10^{-8} mm.

A portion of the beam was intercepted by an aperture plate. This aperture plate was attached to the anode on the side away from the cathode. Figure VII-5 indicates the effect of the interception current on the noise measurements. Even though the noise-current minima were raised as a result of partition noise, the noise current remained, usually, much below the level that would be predicted by Eq. 1. The noise level as computed from Eq. 1 is indicated by dashed lines.

The effect of interception noise was also determined, with Peter's low-noise three-region gun. Figure VII-6 shows how the noise characteristics were affected when 60-65 percent of the beam was intercepted. The interception was made this time with the aid of an aperture hole in the shutter attached to the movable cavity. The curves of Fig. VII-6 were taken with anode voltages corresponding to (a) the values recommended by Peter and (b) the values at which the standing wave was smoothed out.

It became evident from the data given in Fig. VII-6 that the noise always remained much below the level that was computed from Eq. 1. The noise level calculated from Eq. 1 was again indicated by dashed lines. Thus North's partition noise formula does not seem to apply under the conditions of these experiments.

C. Fried

References

1. R. W. Peter, RCA Review 13, 344-368 (1952).

2. J. R. Pierce, Paper to be published, J. Appl. Phys.

3. H. A. Haus, Sc. D. Thesis, M.I.T. (June 1954).

4. B. J. Thompson, D. O. North, and W. A. Harris, RCA Review 4, No. 3 (1940).

E. LARGE-SIGNAL MEASUREMENTS

The measurements on the movable klystron structure described in the Quarterly Progress Report of January 15, 1954 were continued. The bunching process caused by a velocity-modulation input was studied in a beam in two different geometries. The first geometry employs a large drift tube (2.25 inches, inside diameter) and a thin beam (beam diameter, 0.055 inch) described in the January report. The second geometry involves an expandable telescopic drift tube (0.085 inch, inside diameter) surrounding an electron beam 0.055 inch in diameter.

The telescopic drift tube was mounted by means of hooks on the opposing walls of the movable cavities. The cavities slid inside the large drift tube (inside diameter, 2.25 inches). See Fig. VII-7. The hooks that held the telescopic drift tube in position could be unlatched inside the vacuum by means of a rod-and-cam arrangement and the

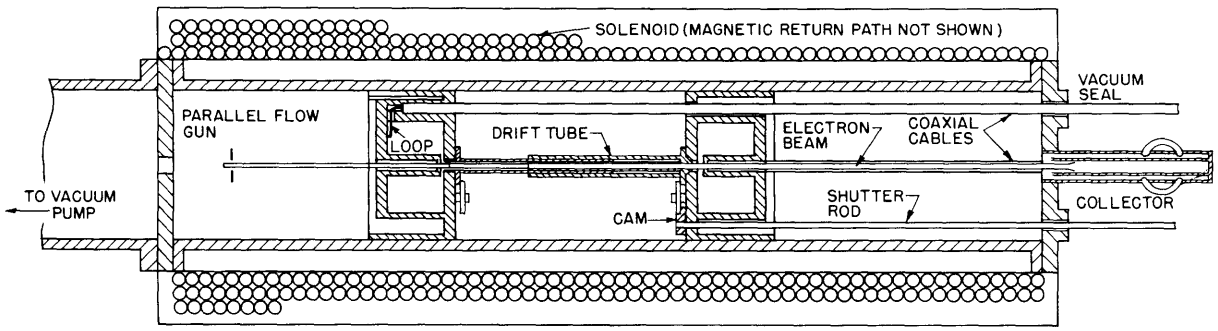

Fig. VII-7
Schematic of beam and drift-tube geometry.

small telescopic drift tube could be dropped to the bottom of the larger drift tube. Thus, the identical measurements could be repeated on the identical beam in two different geometries. The input power to the buncher cavity and the output power from the catcher cavity were measured by TBN-3EV-W thermistor bridges. The accuracy of the power measurements was 0.2 db; the frequency of operation was 3000 Mc/sec.

The catcher cavity was placed at the position of the first current maximum. The output power and the position of the maximum were recorded as functions of the input power in the two geometries. A plot of the experimental data is shown in Fig. VII-8. The power reference level is arbitrary.

From Fig. VII-8 it can be concluded that the plasma wavelength of the beam in the telescopic drift tube (system a) is larger than that of the beam in the large drift tube (system b), as predicted by theory. The standing-wave pattern of system a begins to change, and the position of the maximum starts to shift at a smaller power input to the buncher cavity in system a than in system b. The gain of system b, although smaller at small signal levels than the gain of system a, is constant over a wider range of input and output power than system a. Actually, the constancy of the gain of system b with the output power, as compared with that of system a is even more to the advantage of the former than Fig. VII-8 shows. If it is assumed that the distance between the buncher and catcher gap is kept constant and equal to a quarter of the respective small signal plasma wavelengths, a new plot can be constructed in which the data are corrected for the shift of the current maximum. This plot is shown in Fig. VII-9, which emphasizes the advantage of system b over system a so far as constancy of gain is concerned.

These experiments seemed to indicate that a modification in the conventional klystron design would lead to an improvement of efficiency at constant gain. If the diameter of the drift tube was made several times larger than the beam diameter and the space-charge forces were correspondingly increased, the gain of the klystron, although decreased, would stay constant up to a higher power output level than is the case when

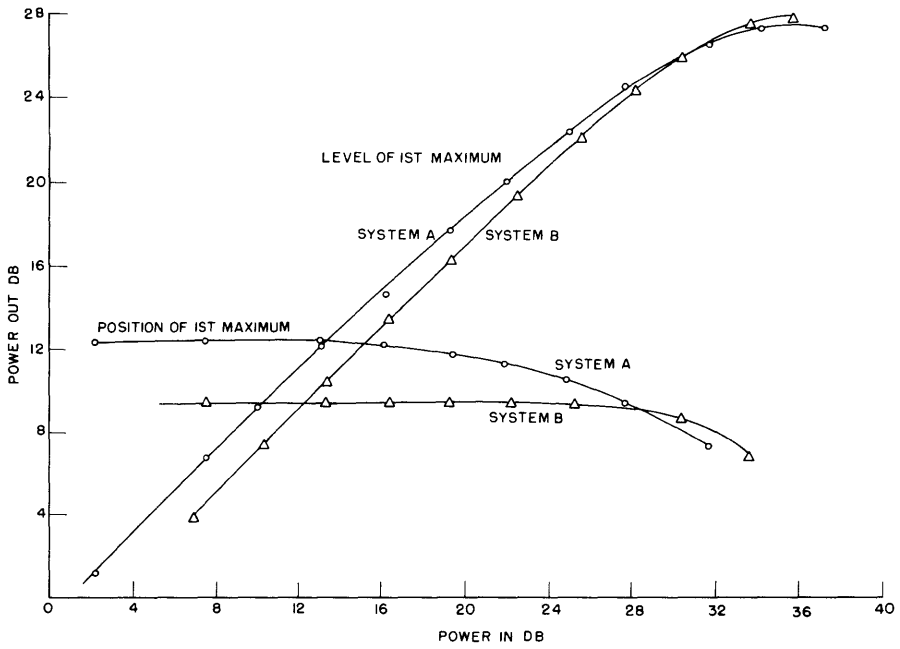

Fig. VII-8

Comparative measurements of the first current maximum in systems a and b.

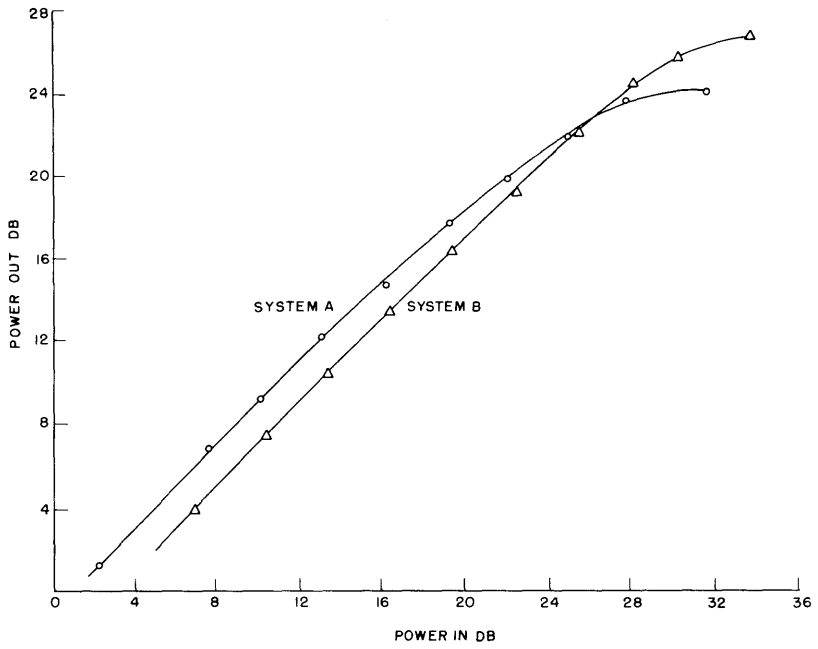

Fig. VII-9

Data of Fig. VII-8 corrected for the shift of the current maximum.

the space-charge forces are kept small by a drift tube closely surrounding the beam.

The importance of the last statement requires further experimental confirmation, since the present experiments were carried out on a beam of small perveance. The gain of the klystron structure was not much above unity. Further experiments will be carried out in the future to determine whether or not the conclusions given above are also valid for beams of high perveance.

H. A. Haus

F. COUPLING OF TWO CONCENTRIC HELICES

Considering two concentric helices as a pair of coupled transmission lines and assuming on them a wave that varies as $\exp(j\omega t - \Gamma z)$, a set of telegrapher's equations may be written

$$\left.\begin{aligned} \Gamma V_1 - jX_1 I_1 - jX_{12} I_2 &= 0 \\ \Gamma I_1 - jB_1 V_1 - jB_{12}(V_2 - V_1) &= 0 \\ \Gamma V_2 - jX_2 I_2 - jX_{12} I_1 &= 0 \\ \Gamma I_2 - jB_2 V_2 - jB_{12}(V_1 - V_2) &= 0 \end{aligned}\right\} \tag{1}$$

from which four values of Γ can be obtained, giving two positive and two negative traveling waves. Each pair of waves interferes in such a manner that power is transferred periodically between the two helices, with the power flow in the direction of the interfering waves.

In order to have complete transfer of power between the two helices in each quarter-beat wavelength two conditions must be met

$$X_1(B_1 - B_{12}) = X_2(B_2 - B_{12}) \tag{2}$$

and

$$\frac{X_{12}}{X_1 X_2} \approx \frac{B_{12}}{B_1 B_2} \quad \text{or} \quad \frac{X_{12}}{X_1 X_2}\frac{B_{12}}{B_1 B_2} \ll 1 \tag{3}$$

With some manipulation condition 2 gives a relation between the phase velocities on the two helices

$$v_2^2 = v_1^2\left[1 + \frac{b(Z_1 - Z_2)}{Z_{mean}}\right] \tag{4}$$

where v is the velocity, Z is the impedance, and b is the normalized mutual susceptance.

$$b \approx \frac{B_{12}}{B_1 B_2} \tag{5}$$

As in Eq. 1, the subscripts 1 and 2 relate to helices 1 and 2, where helix 1 will be denoted as the inner helix. Since b is negative, and $Z_1 > Z_2$, v_2 turns out to be slightly smaller than v_1. This small difference is very critical, however, for transfer of power and directivity of power flow. In Fig. VII-10 a comparison of the directivity for two helices with equal phase velocities and two helices with the phase velocities determined from Eq. 4 is shown.

Condition 3 can be met most easily in practice by making the coupling between the helices loose. Since the fields around the helices decay quite rapidly, a ratio of diameter of 2 to 1 is more than adequate.

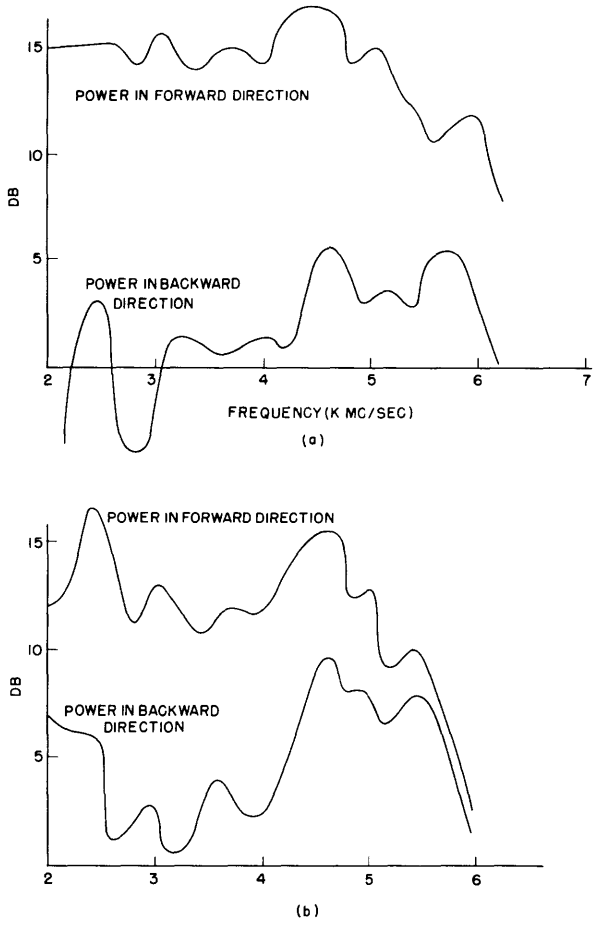

Fig. VII-10

Directivity properties of two helices:
(a) correct phase velocity conditions;
(b) equal phase velocities.

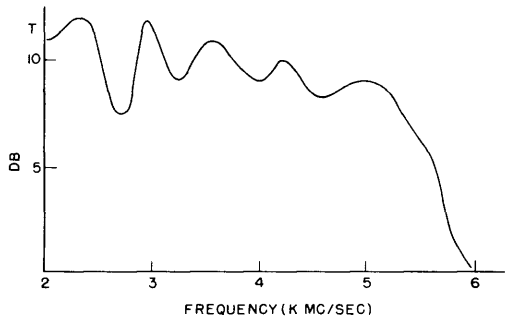

Fig. VII-11

Transmitted power vs frequency.

Another condition that must be met for power coupling is that the coupling helix must be of a diameter that is small enough to be well below the forbidden regions of Sensiper's analysis at the highest frequencies used. This condition can be shown to be

$$\lambda > 2\pi a(1 + \sin \Psi) \tag{6}$$

where λ is the free-space wavelength, a is the radius of the helix, and Ψ is the helical angle. For the experimental coupling, the cut-off frequency was found to be 6.4 kMc/sec. The experimentally determined transmitted power began to fall off sooner than predicted, as shown in Fig. VII-11. This makes the limitation on the coupling helix diameter even more stringent than that given by Eq. 6.

The discrepancy between theoretical calculation of the beat wavelength by the sheath helix approximation and the experimentally determined beat wavelength (see the Quarterly Progress Report of January 15, 1954) has been partly resolved. This was done by considering corrections for the presence of a shield around the coupling helix and the fact that the structures were real wire helices rather than sheath helices. The presence of dielectric was found to have little effect other than that caused by the change in phase velocities.

The use of Tien's helix impedance reduction factor closely accounted for the discrepancy between the experimental and theoretical determinations of the beat wavelength. The theoretical justification of its use, however, is somewhat questionable. The effect of the outer shield can be taken into account by a quasi-static approach (2) to find the reduction in field strengths. This quantitatively accounts for the lengthening of the beat wavelength that results from the presence of the shield.

A. J. Lichtenberg

References

1. P. K. Tien, Proc. I.R.E. 41, 1617 (1953).

2. A. J. Lichtenberg, M.Sc. Thesis, M.I.T., June 1954.